Thermal stability and electrical transport properties of Ge/Sn-codoped single crystalline β-Zn_4Sb_3 prepared by the Sn-flux method*

Hong-xia Liu(刘虹霞)[1], Shu-ping Deng(邓书平)[1], De-cong Li(李德聪)[2], Lan-xian Shen(申兰先)[1], and Shu-kang Deng(邓书康)[1,†]

[1] *Education Ministry Key Laboratory of Renewable Energy Advanced Materials and Manufacturing Technology, Yunnan Normal University, Kunming* 650500, *China*

[2] *Photoelectric Engineering College, Yunnan Open University, Kunming* 650500, *China*

(Received 15 September 2016; revised manuscript received 23 November 2016; published online 20 December 2016)

This study prepares a group of single crystalline β-Zn_4Sb_3 with Ge and Sn codoped by the Sn-flux method according to the nominal stoichiometric ratios of $Zn_{4.4}Sb_3Ge_xSn_3$ ($x = 0$–0.15). The prepared samples possess a metallic luster surface with perfect appearance and large crystal sizes. The microscopic cracks or defects are invisible in the samples from the back-scattered electron image. Except for the heavily Ge-doped sample of $x = 0.15$, all the samples are single phase with space group $R\bar{3}c$. The thermal analysis results show that the samples doped with Ge exhibit an excellent thermal stability. Compared with the polycrystalline Ge-substituted β-Zn_4Sb_3, the present single crystals have higher carrier mobility, and hence the electrical conductivity is improved, which reaches 7.48×10^4 S·m^{-1} at room temperature for the $x = 0.1$ sample. The change of Ge and Sn contents does not improve the Seebeck coefficient significantly. Benefiting from the increased electrical conductivity, the sample with $x = 0.075$ gets the highest power factor of 1.45×10^{-3} W·m^{-1}·K^{-2} at 543 K.

Keywords: thermoelectric materials, β-Zn_4Sb_3, flux method, electrical transport properties

PACS: 74.25.fg, 74.25.fc, 81.10.–h **DOI:** 10.1088/1674-1056/26/2/027401

1. Introduction

Thermoelectric material has become a promising functional material with its unique performance to achieve transformation between heat and electricity including thermoelectric generation and refrigeration. High cost and low thermoelectric conversion efficiency has been limiting the extensive application of thermoelectric materials for a long time in the past.[1–3] The thermoelectric properties are characterized by the dimensionless thermoelectric figure of merit — ZT, $ZT = \alpha^2\sigma T/\kappa$, where α, σ, and κ are respectively the Seebeck coefficient, electrical conductivity and thermal conductivity of materials, T is the absolute temperature. The goals to develop and research new thermoelectric materials lie in the efforts to increase the electrical conductivity, Seebeck coefficient, and reduce the thermal conductivity simultaneously of the materials.[4,5]

β-Zn_4Sb_3, a novel p-type thermoelectric material with a high ZT value (1.40 at 675 K) in the medium temperature area (473 K–673 K), has aroused extensive attention.[6–9] The high TE performance of β-Zn_4Sb_3 mainly originates from the intrinsically low thermal conductivity for the complex and disordered crystal structure (about 0.65 W·m^{-1}·K^{-1} of lattice thermal conductivity at room temperature).[10] Besides that, the component elements are low-cost and environmentally friendly. In order to further improve the ZT, the current Seebeck coefficient and electrical conductivity are relatively lower and should be improved. Besides the production methods, doping is a feasible approach to improve the thermoelectric properties which regulates the electronic structures and adjusts the carrier concentration.[11,12] In the past years, elements in the vicinity of Zn and Sb such as In, Pb, Sn, Cd, Bi, Mg, etc. were generally selected to dope the β-Zn_4Sb_3,[13–20] but Ge-substitution in β-Zn_4Sb_3 has been rarely reported so far. Wang *et al.* recently demonstrated the realization of a high thermoelectric figure of merit in Ge-substituted β-Zn_4Sb_3, the experimental results and theoretical calculations revealed that Ge substitution had a marked improvement on the Seebeck coefficient and the power factor.[21] However, the reported poor stability and weak mechanical property of polycrystalline β-Zn_4Sb_3 due to many micro-cracks or phase decomposition limit the practical applications.[22,23] Recently our work showed that β-Zn_4Sb_3 single crystals with superior performance can be obtained by the Sn-flux method,[24] and the stability of single crystalline β-Zn_4Sb_3 was improved compared with that of polycrystals.[25] In order to explore the effects of Ge substitution on the structure and properties of β-Zn_4Sb_3 single crystals, in this paper, Ge was doped in the β-Zn_4Sb_3 prepared by using the Sn-flux method, and Sn was inevitably incorporated in the synthesis process, so the Ge/Sn codoped single crystalline β-Zn_4Sb_3 were obtained. The influence of Ge/Sn codoping on the thermal stability and electrical transport properties has been investigated.

*Project supported by the National Natural Science Foundation of China (Grant No. 51262032).

†Corresponding author. E-mail: skdeng@126.com

© 2017 Chinese Physical Society and IOP Publishing Ltd

2. Experimental

Ge/Sn codoped single crystalline β-Zn_4Sb_3 samples were prepared by using the Sn-flux method combined with melting and slow cooling technology. The high-purity elements of Zn (grains, 99.999%), Sb (grains, 99.999%), Ge (ingots, 99.999%), and Sn (grains, 99.999%) were weighed according to the stoichiometric ratios of Zn:Sb:Ge:Sn = 4.4:3:x:3 ($x = 0$, 0.03, 0.05, 0.075, 0.1, 0.15) as raw materials, the slightly additional Zn in the raw materials was aimed to compensate for the Zn loss during the synthesis process because of the relatively higher saturated vapor pressure of Zn. The weighed mixtures were loaded into quartz ampoules and sealed after evacuation. The quartz ampoules were then placed in a box furnace and heated to 853 K for 2 h. The mixture was held at this temperature for 12 h, and then cooled to 753 K for 15 min, followed by cooling to 593 K for 40 h. The mixture was held at this temperature before the molten flux was separated from the mixture by centrifugation.

The crystalline structure and phase were characterized by x-ray diffractometer (XRD; Ultima IV). The chemical compositions and back-scattered electron image (BSI) of the samples were obtained by electron probe microanalysis (EPMA; JXA-8230); when analyzing the actual content of each element, the average value of ten test points across the sample was gained for the same sample. The Hall coefficient R_H at room temperature of the single crystalline β-Zn_4Sb_3 samples were measured using the Hall measurement system (Nanometrics HL5500 Hall System) in 0.55-T magnetic fields. The melting point and thermal stability were measured by the thermogravimetric-differential thermal analysis (TG-DSC; STA449F3 Jupiter) in open alumina crucibles with a heating rate of 10 K/min and high-purity nitrogen was used as purge gas. The electrical conductivity σ and the Seebeck coefficient α were measured from 300 K to 660 K in a vacuum. When measuring the Seebeck coefficient, Konstantan (Ni: 40%) was used as a reference sample with a temperature difference maintained below 2 K. The Seebeck coefficient α of the samples was calculated using the formula $\alpha = \Delta E/\Delta T$, where ΔE is the electric potential. The electrical conductivity σ of the samples was measured using the direct current (DC) four probe method with 20-mA DC.

3. Results and discussion

3.1. Structure, compositions and thermal analysis of samples

The crystal growth results show that the introduction of slight Ge can yield perfect single crystals. As an example, the morphology image and BSI of the x = 0.075 sample are shown in Fig. 1. From Fig. 1(a), the Ge/Sn-codoped single crystalline β-Zn_4Sb_3 possesses a metallic luster surface and regular shape with a crystal size of 8 mm. Combining with the internal back scattering image of the polished surface obtained by EPMA in Fig. 1(b), the microscopic cracks or defects are invisible at 40 times magnification which indicates the crystals should have good mechanical properties. Therefore, the present single crystalline β-Zn_4Sb_3 shows a significant advantage over the β-Zn_4Sb_3 polycrystals prepared by traditional melting with microcracks.

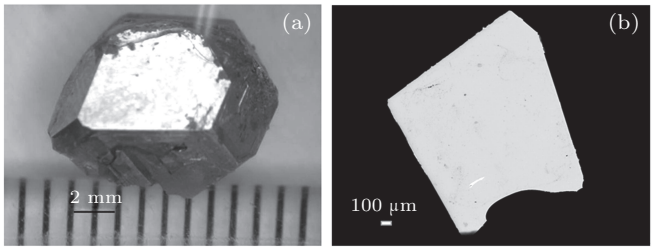


Fig. 1. The morphology (a) and back-scattered electron image (BSI) (b) of the single crystal sample with the nominal composition of $Zn_{4.4}Sb_3Ge_{0.075}Sn_3$ prepared by Sn-flux method.

The sample phase compositions were identified by powder XRD shown in Fig. 2(a). The diffraction peaks of the samples except for the most heavily Ge-doped sample of $x = 0.15$ correspond well to the standard card of PDF #34-1013, which can be identified as a single β phase with space group $R\bar{3}c$. With regard to the $x = 0.15$ sample, a ZnSb second phase can be detected due to the excessive Ge. However, no Ge-associated impurity phase was detected.

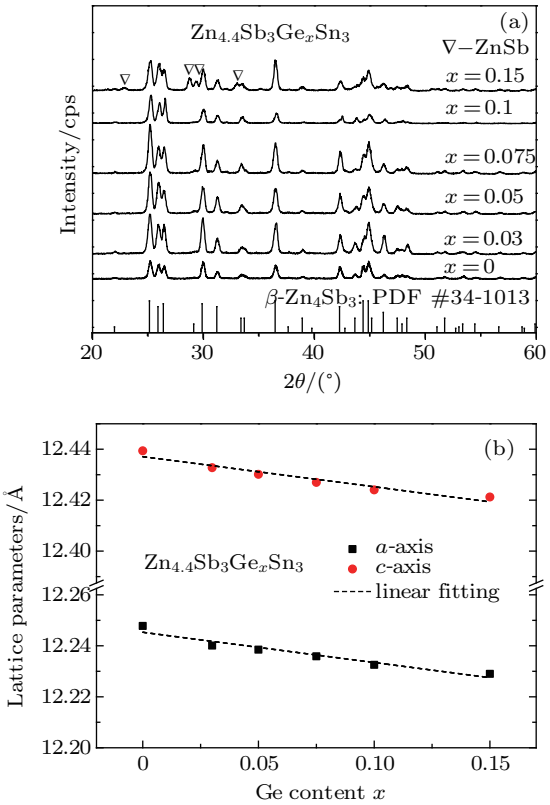


Fig. 2. (color online) Powder XRD patterns of the samples (a) and lattice parameters as a function of Ge content x (b) prepared by Sn-flux method based on the nominal stoichiometric ratios of $Zn_{4.4}Sb_3Ge_xSn_3$ ($x = 0$–0.15).

The actual compositions of all the samples are listed in Table 1. For comparison, the EPMA composition was normalized to antimony atom. As we can see, both Ge and Sn

prefer to substitute for Zn, and only a small amount of Ge is incorporated which indicates a small solid solubility of Ge in the compound, which is lower than the experimental results reported by Wang *et al.*[21] It may be caused by the lower melting reaction temperature. For another reason, the starting Ge distributed in the Sn flux, thus, the lower ratio of Ge in the reactants lead to smaller Ge content. The content of Sn is decreased with the increase of Ge, it is believed that the increase of Ge in the melt increases the melting/crystallization temperature that leads to the decrease of Sn in the crystals (Table 1). The dependence of lattice parameters on Ge content in Fig. 2(b) shows that both *a* and *c* axes of Ge/Sn-codoped samples decreased obviously mainly due to the decrease of the amount of the Sn atom. Compared with the reported values,[14,16,18,21] the lattice parameters of the sample without Ge substitution are larger due to the larger incorporation of Sn with a larger atomic radius.

Table 1. Actual compositions, carrier concentration n, Hall coefficient R_H, and carrier mobility μ_H at room temperature for single crystalline β-Zn_4Sb_3 samples prepared using the Sn flux method based on the nominal stoichiometric ratios of $Zn_{4.4}Sb_3Ge_xSn_3$ ($x = 0$–0.15).

Nominal compositions of Ge	Actual compositions				$n/10^{19}$ cm^{-3}	$R_H/10^{-8}$ m^3·C^{-1}	μ_H/cm^2·V^{-1}·s^{-1}
	Zn	Sb	Ge	Sn			
$x = 0$	3.82	3	0	0.084	5.48	11.4	78.85
$x = 0.03$	3.77	3	0.0034	0.0678	6.93	9.015	58.20
$x = 0.05$	3.76	3	0.0035	0.0676	4.71	13.28	81.05
$x = 0.075$	3.74	3	0.0038	0.0642	6.93	9.017	66.20
$x = 0.1$	3.74	3	0.0043	0.0627	5.56	11.238	84.07
$x = 0.15$	3.75	3	0.0049	0.0509	9.55	6.543	51.69

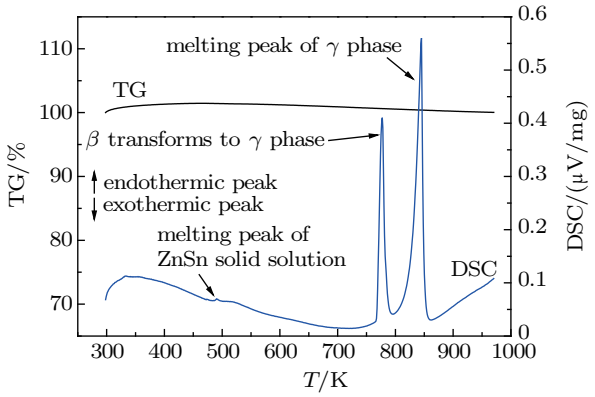


Fig. 3. (color online) Thermal analysis of sample with $x = 0.075$ prepared by the Sn-flux method according to the nominal formula of $Zn_{4.4}Sb_3Ge_xSn_3$ ($x = 0$–0.15) performed in open alumina crucibles with a heating rate of 10 K/min and high-purity nitrogen was used as purge gas and protective gas.

Figure 3 is the thermal analysis result of the $x = 0.075$ sample. As with the β-Zn_4Sb_3 sample without Ge-doping prepared by Sn-flux method,[24] the present single crystalline samples still exhibit an unexceptional thermal stability. From the TG curve, there is no weight loss below the melting temperature for the present sample which indicates the doped Ge does not have a negative impact on the thermal stability. As for the temperature dependence of DSC, the tiny endothermic peak at 490 K can be identified as the melting peak of Zn–Sn eutectic compound which is not completely separated from the surface of single crystals. The phase transformation of β to γ phase started from 768 K, which is in accordance with that of 767 K shown in the phase diagram.[26] The endothermic peak at 845 K is the melting peak of the sample, and the melting point is about 829 K, which is lower than that of the 837 K of Zn_4Sb_3 compound shown in the phase diagram;[26] this finding may be caused by the doped Sn with lower melting point. Finally, as seen from DSC curve, there are no other thermal decomposition peaks appearing, which is consistent with the thermogravimetric analysis result. It is believed that the perfect crystals with fewer vacancy defects contribute to the superior thermal stability in this study.

3.2. Electrical transport properties

The Hall coefficient R_H was measured at room temperature to determine the electrical properties, and the carrier concentration n, and carrier mobility μ_H were obtained from the measured R_H and σ at 300 K using the equations, $n = 1/(e|R_H|)$ and $\mu_H = |R_H| \times \sigma$, respectively, where e is the electron charge (Table 1). All the Hall coefficients are positive, indicating the prepared single crystalline samples exhibit a p-type conductivity. The carrier concentration is of the order of 10^{19} cm^{-3}, which corresponds to heavily doped semiconductors, and it is consistent with the optimal carrier concentrations reported by Snyder *et al.*[27] The carrier concentration of the $x = 0.15$ sample is higher for the appearance of narrow energy gap ZnSb phase which reduces its ionized energy.

Figure 4 shows the temperature dependence of the electrical conductivity for all β-Zn_4Sb_3 samples. The electrical conductivity which decreased monotonously with the increasing temperature except for the $x = 0.15$ sample, exhibits a degenerate semiconductor transport behavior. The electrical conductivity of the $x = 0.1$ sample reaches the value of $7.48\times\ 10^4$ S·m^{-1} at room temperature, which improves by 8% compared with the Ge unsubstituted sample due to the increasing carrier concentration. Furthermore, it is also higher than the value of the 1.0 at.% Ge-substituted polycrystalline β-Zn_4Sb_3 reported by Wang *et al.* which reaches about 5.5×10^4 S·m^{-1} at 300 K.[21] The improvement of electrical conductivity for the single crystals can be attributed to

the higher mobility than that of polycrystals,[21] for the single crystals have naturally low grain boundary scattering due to the effect of grain boundary. In the case of $x = 0.15$, the emergence of ZnSb second phase greatly influences the material phase structure, and the electrical conductivity demonstrates a remarkable intrinsic conduction at 573 K.

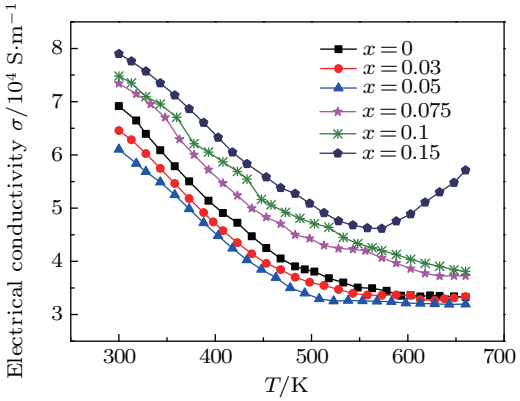


Fig. 4. (color online) The temperature dependence of the electrical conductivity for all β-Zn_4Sb_3 samples prepared using the Sn-flux method based on the nominal stoichiometric ratios of $Zn_{4.4}Sb_3Ge_xSn_3$ ($x = 0$–0.15).

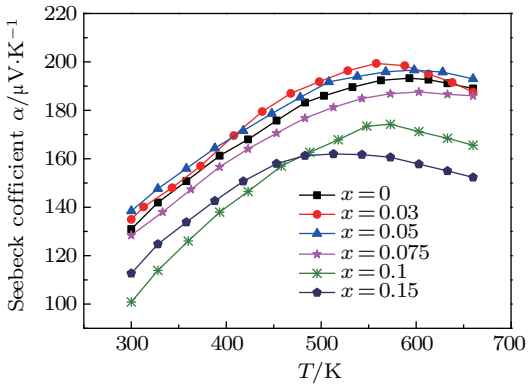


Fig. 5. (color online) The temperature dependence of the Seebeck coefficient for all β-Zn_4Sb_3 samples prepared using the Sn-flux method based on the nominal stoichiometric ratios of $Zn_{4.4}Sb_3Ge_xSn_3$ ($x = 0$–0.15).

The temperature dependence of the Seebeck coefficient for all β-Zn_4Sb_3 samples is shown in Fig. 5. The positive Seebeck coefficients again demonstrate that the major charge carriers in all the samples are holes. As seen from the Seebeck coefficient of the prepared samples, the change of the Ge and Sn content does not improve the α significantly. The Seebeck coefficient of the Ge/Sn codoped samples with $x = 0.03$ and 0.05 exhibited a similar temperature behavior to the non-Ge β-Zn_4Sb_3. The highest value of 199 μV·K^{-1} is attained at 558 K for the $x = 0.03$ sample, which is comparable to previous reported values.[13,21] Then the Seebeck coefficient decreased with the increased Ge doping amount, presumably this behavior can be ascribed to the fact that the excessive Ge or the decrease of Sn have some influence on the band structure of the compounds.

Figure 6 shows the temperature dependence of the power factor which was calculated by the formula of $P = \alpha^2\sigma$. Benefiting from the increased electrical conductivity, the $x = 0.075$ sample gets the highest power factor of 1.45×10^{-3} W·m^{-1}·K^{-2} at 543 K, which is comparable to the highest value of 0.25 at.% Ge-substituted β-Zn_4Sb_3 polycrystal (1.4×10^{-3} W·m^{-1}·K^{-2} above 500 K).[21]

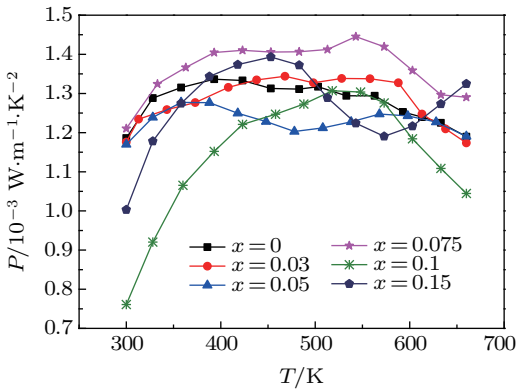


Fig. 6. (color online) The temperature dependence of the power factor for all β-Zn_4Sb_3 samples prepared using the Sn-flux method based on the nominal stoichiometric ratios of $Zn_{4.4}Sb_3Ge_xSn_3$ ($x = 0$–0.15).

4. Conclusions

In this paper, Ge/Sn codoped single crystalline β-Zn_4Sb_3 with space group $R\bar{3}c$ was prepared according to the nominal stoichiometric ratios of $Zn_{4.4}Sb_3Ge_xSn_3$ ($x = 0$–0.15). The prepared samples possessed perfect morphology and large crystal sizes. The microscopic cracks or defects are invisible in the samples from the back-scattered electron image, showing a significant advantage over the β-Zn_4Sb_3 polycrystals prepared by traditional melting method. The Ge/Sn-codoped single crystalline samples show a good thermal stability. All the samples exhibit p-type conduction. The electrical conductivity is increased compared with the non-Ge sample, while the Ge substitution does not improve the α significantly. The samples with Ge/Sn-codoped possess good electrical transport properties with the highest power factor of 1.45×10^{-3} W·m^{-1}·K^{-2} at 543 K for the $x = 0.075$ sample.

References

[1] Lin J, Li X, Qiao G, Wang Z, Carrete J, Ren Y, Ma L, Fei Y, Yang B, Lei L and Li J 2013 *J. Am. Chem. Soc.* **136** 1497
[2] Meng D Y, Shen L X, Shai X X, Dong G J and Deng S K 2013 *Acta Phys. Sin.* **62** 247401 (in Chinese)
[3] Zhang Y, Wu L H, Zengli J K, Liu Y F, Zhang J Y, Xing J J and Luo J 2016 *Acta Phys. Sin.* **65** 107201 (in Chinese)
[4] Slack G A 1995 in *CRC handbook of thermoelectrics*, ed. Rowe D M (Boca Raton, FL: CRC Press) p. 407
[5] Wang J S, Cheng F, Liu H X, Li D C, Shen L X and Deng S K 2016 *Chin. Phys. B* **25** 067402
[6] Toberer E S, Rauwel P, Gariel S, Taftø J and Snyder G J 2010 *J. Mater. Chem.* **20** 9877
[7] Snyder G J, Christensen M, Nishibori E, Caillat T and Iversen B B 2004 *Nat. Mater.* **3** 458
[8] Mozharivskyj Y, Janssen Y, Harringa J L, Kracher A, Tsokol O A and Miller G J 2006 *Chem. Mater.* **18** 822
[9] Ur SC, Kim IH and Nash P 2004 *Mater. Lett.* **58** 2132
[10] Caillat T, Fleurial J P and Borshchevsky A 1997 *J. Phys. Chem. Solids* **58** 1119
[11] Tan G, Wang S, Li H, Yan Y and Tang X 2012 *J. Solid State Chem.* **187** 316

[12] Nong N Van, Pryds N, Linderoth S and Ohtaki M 2011 *Adv. Mater.* **23** 2484
[13] Shai X, Deng S, Shen L, Meng D, Li D, Zhang Y and Jiang X 2015 *Phys. Status Solidi B* **252** 795
[14] Wang S Y, She X Y, Zheng G, Fu F, Li H and Tang X F 2012 *J. Electron. Mater.* **41** 1091
[15] Koyanagi T, Hino K, Nagamoto Y, Yoshitake H and Kishimoto K 1997 *IEEE XVI International Conference on Thermoelectrics* 463
[16] Wang S, Fu F, She X, Zheng G, Li H and Tang X 2011 *Intermetallics* **19** 1823
[17] Pedersen B L, Yin H, Birkedal H, Nygren M and Iversen B B 2010 *Chem. Mater.* **22** 2375
[18] Qin X Y, Liu M, Pan L, Xin H X, Sun J H and Wang Q Q 2011 *J. Appl. Phys.* **109** 033714
[19] Nakamoto G, Tajima Y and Kurisu M 2012 *Intermetallics* **23** 163
[20] Pedersen B L, Birkedal H, Nygren M, Frederiksen P T and Iversen B B 2009 *J. Appl. Phys.* **105** 382
[21] Wang S, Tan X, Tan G, She X, Liu W, Li H, Liu H and Tang X 2012 *J. Mater. Chem.* **22** 13977
[22] Mozharivskyj Y, Janssen Y, Harringa J L, Kracher A, Tsokol A O and Miller G J 2006 *Chem. Mater.* **18** 822
[23] Zhang L T, Tsutsui M, Ito K and Yamaguchi M 2003 *J. Alloys Compd.* **358** 252
[24] Shai X, Deng S, Meng D, Shen L and Li D 2014 *Physica B: Condens. Matter* **452** 148
[25] Liu H, Deng S, Li D, Shen L, Cheng F, Wang J and Deng S 2016 *Physica B: Condens. Matter* **500** 9
[26] Okamura C, Ueda T and Hasezaki K 2010 *Mater. Trans.* **51** 152
[27] Snyder G J and Toberer E S 2008 *Nat. Mater.* **7** 105